DOI: https://doi.org/10.31351/vol32iss3pp105-117

Preparation and *in vitro* Evaluation of Synthetic High-Density Lipoproteins as Parenteral Drug Delivery System for Tamoxifen Citrate

Ameerah A. Radhi*[,1], Wedad K. Ali[1] and Fitua Al-Saedi [2]

[1]Department of Pharmaceutics, College of Pharmacy, Mustansiriyah University, Baghdad, Iraq.
[2]Department of Clinical Laboratory Sciences, College of Pharmacy, Mustansiriyah University, Baghdad, Iraq.

Abstract

The aim of this study was to develop a bioinspired drug delivery system for tamoxifen citrate (TC) based on synthetic high density lipoproteins (sHDL). For this purpose, sHDL nanoparticles were prepared from a mimetic peptide (5A peptide) and different lipids using thin film hydration method followed by sonication and thermal cycling. Various formulation parameters including lipid composition, lipid to peptide ratio, and drug to carrier ratio had a remarkable impact on the properties and the release pattern of the nanoparticles. The optimized formula (F14) displayed a spherical morphology, average diameter of (35.7±12.4) nm, and a zeta potential (ζ) equals to (-48.4± 0.5) mV. The encapsulation efficiency and drug loading of F14 were (96.5±0.7%) and (9.65±0.1%), respectively. Besides, F14 showed a good stability in human plasma for 24 hours. The encapsulation of the lipophilic drug within the hydrophobic core of the nanocarrier enabled a slow drug release from nanoparticles which follows a near zero order controlled mechanism. The promising results of this study open an avenue for using sHDL as a delivery system for administration of TC intravenously. Therefore, the optimized formula is suggested to be a subject for future analyses in terms of *in vitro* cytotoxicity against breast cancer cells and *in vivo* evaluation in tumor bearing animals.

Keywords: Tamoxifen citrate, Breast cancer, Bioinspired drug delivery system, Synthetic high density lipoproteins, Mimetic peptide.

التحضير والتقييم المختبري للبروتينات الدهنية المصنَعة العالية الكثافة كنظام ناقل لدواء التاموكسفين سترات عن طريق الزرق

اميره عبدالاله راضي*[،١]، وداد كمال علي[١] و فتوة منور عزيز[**]

[١]فرع الصيدلانيات ، كلية الصيدلة ، الجامعة المستنصرية ، بغداد ، العراق.
[٢] فرع العلوم المختبرية السريرية ، كلية الصيدلة ،الجامعة المستنصرية، بغداد، العراق.

الخلاصة

إنَّ الهدف من هذه الدراسة هو تطوير نظام ناقل مستوحى من النظام الأحيائي لتوصيل دواء التاموكسفين سترات من البروتينات الدهنية المصنَعة عالية الكثافة.لتحقيق هذا الغرض تم تحضير البروتينات الدهنية عالية الكثافة باستخدام ببتيد محاكي ودهون مختلفة بطريقة ترطيب الأغشية الرقيقة متبوعاً بالموجات فوق الصوتية والتبادل الحراري. كان لعوامل التحضير المشتملة على المكونات الدهنية , نسبة الدهون :الببتيد، نسبة الدواء :الحامل النانوي الأثر الفاعل على الخصائص المختلفة ونمط تحرر الدواء من الجسيمات النانوية. أظهرت الصيغة المثالية (F14) شكلاً كروياً و معدل حجم يبلغ 35.7±12.4 نانوميتر , جهد زيتا 48.4±0.5- ملي فولت. كفاءة احتجاز تبلغ 96.5±0.7% وكفاءة تحميل تساوي 9.65±0.1% . كما أظهرت استقرارا حين مزجها مع بلازما الانسان لمدة ٢٤ ساعة. إنَّ إحتجاز الدواء المحب للدهون ضمن اللب الدهني للحامل النانوي مكَّن من إبطاء تحرر الدواء بنمط يخضع لحركية المرتبة الصفرية . إنَّ النتائج الواعدة لهذه الدراسة تفتح الطريق أمام إستخدام البروتينات الدهنية المصنَعة عالية الكثافة كنظام ناقل لدواء التاموكسفين سترات يمكن اعطاؤه عن طريق الزرق. لذلك نقترح إخضاع الصيغة المثالية لتحاليل مستقبلية تتضمن التقييم المختبري للسمية الخلوية ضد خط خلايا سرطان الثدي بالإضافة الى التقييم داخل الجسم الحي للحيوانات المختبرية.

الكلمات المفتاحية:تاموكسفين سترات،سرطان الثدي، نظام ناقل مستوحى من النظام الأحيائي ، البروتينات الدهنية المصنَعة عالية الكثافة، ببتايد محاكي.

Introduction

Breast cancer (BC) is one of the most common types of cancer and ranked the second cause of cancer mortality in women following lung cancer [(1)]. Tamoxifen citrate (TC) is the standard endocrinetherapy for estrogen receptor (ER) positive breast cancer in premenopausal women for nearly four decades[(2)]. TC is the trans isomer of atriphenylethylene derivative, chemically designated as 2 - [4 - [(Z)-1,2-Diphenylbut-1-enyl] phenoxy]-N, N-dimethylethanamine dihydrogen 2-hydroxypropane-1,2,3-tricarboxylate[(3)].

It is a weak base with a dissociation constant (pKa) of 8.85; and has a highly lipophilic nature with value of partition coefficient (Log P) equals to 5.93[(4).] It has melting point of 140-142ºC, and it is slightly soluble in water and in acetone, but soluble in methanol [(5)].

Tamoxifen is defined pharmacologically as a selective estrogen receptor modulator (SERM); tamoxifen demonstrates antagonist effect on the breast and agonist effect on other tissues such as

*Corresponding author E-mail: ameerahradhi@uomustansiriyah.edu.iq
Received: 8/ 10/ 2022
Accepted: 28/12 /2022

uterus and bones[6]. The drug's antagonist (anti-estrogen) effect has succeeded in decreasing the disease recurrence and mortality. Nevertheless, several adverse effects were attributed to its agonist properties including endometrial hyperplasia, polyps, cancer, and increased risk of thromboembolism[7,8]. In this context, it is essential to develop novel strategies that are highly specific to the tumor site. Nano- based drug delivery systems have emerged as a successful approach[9].

Synthetic high density lipoproteins (sHDL) possess most of the advantages of the natural HDL in term of excellent biocompatibility, reticuloendothelial system (RES) escape, and prolonged drug′s circulation. Several sHDL products have been tested in phase I and II clinical trials with over 800 patients, and data revealed that HDL products are well tolerated with no major side effects[10]. Besides, the small size of sHDL facilitates better penetration into tumor tissues. Apolipoprotein A-I (apoA-I), the main apolipoprotein in HDL, possesses an excellent ability to target scavenger receptor class B type I (SR-BI) overexpressed in various kinds of cancer cells including breast cancer. Thus, the delivery of antitumor drugs through the receptor–ligand binding between SR-BI and apoA-I is obviously a promising therapeutic approach[11].

Concerning the drug loading capacity of sHDL, hydrophobic molecules can be passively encapsulated into the core of sHDL. Likewise, amphiphilic drugs are readily inserted into the lipid membrane. The challenging molecules like hydrophilic drugs can be conjugated to a suitable lipophilic functional group to enhance their hydrophobicity as shown in figure (1). The resulting prodrug can be incorporated into the core of sHDL to be later cleaved and release the original therapeutic agent at the target site[12].

Natural HDL exist in two main subclasses, the discoidal and the spherical HDL based on their constituents[13].As previously reported in literature, sHDL formulation comprising phospholipids (with or without cholesterol) and peptides usually leads to formation of discoidal sHDL (also termed as sHDL nanodiscs). On the other hand, the preparation of spherical sHDL usually calls for phospholipids, free cholesterol (FC), peptides, cholesteryl esters (CE), and triglycerides (TG). In this study, both discoidal sHDL and spherical sHDL nanoparticles have been developed [14].

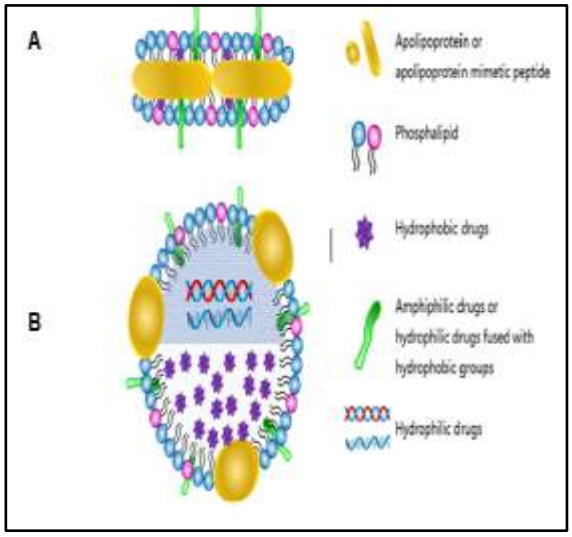

Figure 1. Schematic representation of (A) discoidal and (B) spherical sHDL drug loading capacity[12]

The nanocarrier intended for targeting anticancer agent to the tumor site and administration via intravenous route must fulfill certain criteria. Firstly, it must have maximum retention of the encapsulated drug until it reaches cancer cells, since rapid release of the encapsulated drug in the bloodstream can cause systemic toxicity and compromise the targeting ability of the nanocarrier[15].Secondly, the size of nanoparticles is also a key parameter for efficient targeting; the diameter range of 10-200 nanometer (nm) is favorable for cancer therapy and likely to benefit from the enhanced permeability and retention (EPR) effect driven tumor accumulation[1]. Particles smaller than 10 nm are susceptible to premature excretion by kidneys and leakage from the normal vasculature causing severe toxicities in healthy tissues, whereas particles larger than 200 nm are most likely to be cleared from circulation by phagocytes[16]. Therefore, the aim of this study was to develop a drug delivery system for TC based on sHDL taking into consideration the aforementioned criteria. The phospholipid composition in terms of fatty acid chain length and the degree of saturation; lipids to peptide ratio; and drug to carrier ratio were varied in order to optimize sHDL formulation in terms of the size, homogeneity, and *in vitro* release behavior.

Materials and methods

Materials

Synthesized 5 A, WLKAFYDK VAEKLKE AFPDWAKAAYDKAAEKAKEAA, was purchased from GenScript USA , Inc. Tamoxifen citrate (TC), 1 , 2 - dipalmitoyl – sn - glycerol -3-phosphocholine (DPPC) , egg sphingomyelin (SM), 1,2-dimyristoyl-sn- glycero-3-phosphocholine (DMPC) and free cholesterol (FC) were purchased from Sigma Aldrich,

Germany. Egg yolk lecithin and cholesteryl oleate (CO) were purchased from Shanghai Tunchem Pharm, China.

Preparation of TC loaded sHDL nanoparticles

Tamoxifen citrate loaded sHDL nanoparticles were prepared by the thin film hydration method. Lipids and TC in predetermined quantities (table 1) were dissolved in chloroform: methanol (1:1) volume ratio. The organic solvent was removed by vacuum, and the resulting film was hydrated with phosphate buffer saline buffer (PBS, pH 7.4). Precise amount of 5 A peptide was dissolved in one milliliter (mL) PBS, and mixed with the lipid suspension. Ultrasound radiation was applied to the mixture using probe sonicator intermittently for one minute (min) duration. The mixture was incubated in water bath at 50ºC for 10 min and cooled below phase transition temperature of the phospholipid for 10 min. The temperature was cycled at least three times to form sHDL[17].

Table 1. Composition of TC loaded sHDL nanoparticles

Formula code	sHDL composition	Lipid to peptide ratio	Lipid quantity (mg)	5 A peptide quantity (mg)	TC quantity (mg)
F1	DPPC: 5A:TC	2:1	15	7.5	6.08
F2	SM:5A:TC	2:1	15	7.5	6.08
F3	DMPC:5A:TC	2:1	15	7.5	6.08
F4	DPPC: 5A:TC	1.5:1	15	10	6.08
F5	SM:5A:TC	1.5:1	15	10	6.08
F6	DMPC:5A:TC	1.5:1	15	10	6.08
F7	DPPC: 5A:TC	1:1	15	15	6.08
F8	SM:5A:TC	1:1	15	15	6.08
F9	DMPC:5A:TC	1:1	15	15	6.08
F10	DMPC: SM: 5A:TC	1.5:1	10 mg DMPC,5 mg SM	10	6.08
F11	DMPC: DPPC: 5A:TC	1.5:1	10 mg DMPC,5 mg DPPC	10	6.08
F12	Lecithin:FC:CO:5A: TC (10:5:5:10:6.08)	2:1	10 mg lecithin,5mg FC, 5 mg CO	10	6.08
F13	Lecithin:FC:CO:5A: TC (10:5:5:13.3:6.08)	1.5:1	10 mg lecithin,5mg FC, 5 mg CO	13.3	6.08
F14	Lecithin:FC:CO:5A: TC (20:10:10:20:6.08)	2:1	20 mg lecithin,10 mg FC, 10 mg CO	20	6.08

Characterization of sHDL nanoparticles

Determination of particle size and polydispersity (PDI)

The hydrodynamic diameters and size distribution (polydispersity index) of sHDL were determined by dynamic light scattering system (DLS) using a 90Plus Particle Size Analyzer (Brookhaven Instruments Corporation, USA). Each sample was diluted with equal volume of distilled water (DW), and analyzed at temperature of 25ºC [18].

Determination of zeta potential (ζ)

Each sample was diluted with equal volume of 0.1M KCl solution, then zeta potential measurement was carried out using a zeta plus zeta potential analyzer (Brookhaven Instruments Corporation, USA)[19].

Field emission scanning electron microscope (FESEM)

Field emission scanning electron microscope (FESEM) uses a field emission gun as the source for the electron generation, with electron beam accelerating voltage from 200 V to 30 kV. The electron beam is focused after passing through electromagnetic lenses, and the electron beam scans the surface with the help of scan coils [20].

Samples of about two drops were individually deposited onto a glass slide, and allowed to dry at room temperature. The nanoparticles were coated with gold under vacuum to render them electrically conductive. Then, samples were examined using FESEM (Inspect ™ F50, FEI company, USA) to obtain information with respect to the morphology and the surface characteristics of nanoparticles [21].

Determination of drug encapsulation efficiency (EE) and drug loading (DL)

Samples of four milliliters of TC loaded-sHDL were added to amicon®ultra-4 centrifugal filter device (molecular weight cut off MWCO 10,000Da) and centrifuged at 3000 rpm [22]. The result of the process was the removal of the un-encapsulated drug in the centrifuge tube, and recovery of TC loaded sHDL in the filter device.

Thereafter, methanol was added to break sHDL and dissolve the encapsulated drug to be assayed by ultraviolet (UV) spectroscopy at 277 nm [23] . EE and DL were determined as per the following[24] :

$$EE\% = \frac{\text{mass of TC in nanoparticles}}{\text{original mass of TC}} * 100\%$$

$$DL\% = \frac{\text{mass of TC in nanoparticles}}{\text{mass of nanoparticles}} * 100\%$$

In vitro drug release profile

The release of TC from different sHDL formulations was carried out using the dialysis bag method; sHDL formulation equivalent to 6.08 mg TC was placed in dialysis bag (MWCO 8000-14000 Da). The dialysis bag was then immersed in 100 mL of PBS (pH 7.4) with 2.5% (w/v) tween 80 for 48 hours at stirring speed of 120 rpm and temperature maintained at 37 ± 0.5ºC [25]. At predetermined time points, samples of 5 mL were withdrawn from the release media and replaced with the same volume of fresh PBS to maintain sink condition. The released tamoxifen was quantified by UV spectroscopy at the lambda max of the drug (278) nm and the percentage of drug released was calculated [26].

Analysis of the kinetics of drug release from sHDL nanoparticles

The *in vitro* release data were fitted by different release models summarized in table (2) to describe the mechanism of drug release from sHDL nanoparticles [27].

Table 2. Summary of mathematical models [28]

Zero-order model	$Q_t = Q_0 + K_0\, t$
First-order model	$\text{Log } Q_t = \log Q_0 - K_1\, t/2.303$
Higuchi model	$Q_t/Q_0 = K_H \sqrt{t}$
Korsmeyer–Peppas	$Q_t/Q_0 = K_{KP}\, t^n$

Where Q_t represents the amount of drug released at time t and Q_0 is the initial amount of drug in solution which often equals zero. K_0, K_1, K_H, and K_{KP} are the release rate constants of zero order, first order, Higuchi and Korsmeyer–Peppas, respectively. The release exponent (n) indicates the mechanism of the drug release; When the numerical value of (n) is less than 0.45, a Fickian diffusion is the predominant mechanism of drug release, while $0.45 < n < 0.89$ implies an anomalous (non-Fickian) diffusion. When n equal to 0.89, it refers to Case-II transport, and when $n > 0.89$, it refers to Super case-II transport [28].

Determination of colloidal stability in human plasma

The optimized formula (F14) was added to human plasma at ratio of 1:1 (v/v). The mixture was kept in water bath at 37ºC for 24 hours to simulate the physiologic conditions that sHDL may encounter in blood stream, then changes in the mean particle size, and zeta potential were monitored [29].

Lyophilization of TC loaded sHDL

The optimized formula (F14) was freeze dried at -45ºC/0.07 mbar in Christ (Alpha 1-2 LD plus, Germany) freeze drier. The resulting powder was stored in a tightly closed container for further analysis.

Powder x-ray diffraction (PXRD)

Pure TC, 5A, egg yolk lecithin and the lyophilized powder of F14 were analyzed by powder x-ray diffractometer (XRD-6000, Shimadzu) in order to determine whether TC was incorporated in a crystalline or amorphous state inside the nanoparticles. Samples were grinded into fine powders, packed individually into a sample holder and analyzed. The X- ray tube was Cu (1.54060 A) at 40 kV and 30 mA. The 2θ scan range was performed from 4–60º [30].

Fourier transforms infrared (FTIR) spectroscopy

Briefly, samples of the pure TC, 5A, lecithin and lyophilized F14 were powdered and mixed with potassium bromide and pressed into discs. Then, FT-IR spectra were recorded over a frequency range of 4000–400 cm^{-1} using FT-IR spectrometer (IRAffinity-1, Shimadzu, Japan) [31].

Statistical analysis

Data are expressed as the mean ± standard deviation. Statistical analysis was conducted using Microsoft excel. Unpaired *t*-test and one-way analysis of variance (ANOVA) were used to compare between two and multiple groups, respectively. $P < 0.05$ was considered significantly different.

Results and Discussion

Tamoxifen loaded- sHDL nanoparticles were prepared by the conventional thin film hydration method. The first step involves the formation of liposomal dispersion containing the lipids and the hydrophobic drug TC which is passively encapsulated in the lipid bilayer of the liposomes. Mixing TC-loaded liposomes with the mimetic peptide (5 A peptide) aided by sonication and thermal cycling facilitated the interaction between peptide and the lipid bilayers. Peptide monomers adsorb to the surface of liposomes, partition and insert themselves into the bilayer followed by stripping of lipid layers and assembly of sHDL. The phase transition temperature (T_m) of phospholipid is the temperature at which a lipid transit from the rigid gel ordered phase to the liquid crystalline state. At this point, the membrane will be in a disordered state with packing defects, thereby allowing the initial peptide insertion into the lipid bilayer [32].

Table 3. Physicochemical characterization of TC loaded sHDL

Formula code	Particle diameter (nm)	PDI	Zeta Potential (mV)	Encapsulation efficiency (EE%)	Drug loading (DL%)
F1	295.5±7.5	0.257±0.12	-51.97±0.8	98.17±1.3	26.13±0.32
F2	253.1 ±5	0.316±0.01	-74.17±1.0	98.83±2.0	26.3±0.25
F3	175.5±2.5	0.3±0.01	-22.98±0.78	99.75±1.7	26.5±0.17
F4	254.4±6.5	0.005±0.02	-55±0.58	98.93±0.9	23.7±0.16
F5	198.7±7.4	0.005±0.01	-45.16±1.9	98.9±0.8	23.74±0.1
F6	159.8±8.6	0.383±0.03	-48.3±1.7	97.9±1.2	23.5±0.24
F7	548.9±20.9	0.383±0.12	-1.62±0.45	97.5±1.2	19.5±0.32
F8	685.2±16.4	0.223±0.09	-6.28±0.2	96.2±2.0	19.24±0.2
F9	438.1±11.3	0.405±0.06	-47.94±0.57	99.5±1.2	19.9±0.38
F10	110.6±4.5	0.005±0.02	-16.27±0.7	96.3±0.9	23.1±0.16
F11	319.2±6.5	0.005±0.001	-44.91±1.21	97.2±1.2	23.3±0.24
F12	77.7±5.7	0.005±0.001	-30.5±1.3	89.2±1.3	17.84±0.32
F13	118.5±6.4	0.509±0.12	-16.2±1.0	95.5±0.9	17.2±0.08
F14	35.7±12.4	0.277±0.02	-48.4±0.5	96.5±0.7	9.65±0.1

Optimization and characterization of TC loaded sHDL nanodiscs

Synthetic HDL composition was optimized to match the size of the natural HDL. Three types of phospholipids were investigated including dipalmitoyl phosphatidylcholine (DPPC), dimyristoyl phosphatidylcholine (DMPC), and egg sphingomyelin (SM). The implemented phospholipids have different hydrocarbon chain length, degree of saturation and phase transition temperature (T_m). DPPC (T_m 41ºC) and DMPC (T_m 23ºC) are synthetic fully saturated phospholipids, while egg SM is a naturally occurring lipid with mostly saturated fatty acids and has T_m of 38ºC [33].

F1, F2 and F3 were prepared with different lipid component but at similar (lipid to peptide) ratio in order to examine the effect of the phospholipid composition on the average diameter of the prepared sHDL. The hydrodynamic diameters and size distribution (polydispersity index) of sHDL were determined by DLS. As shown in table 3, F3 (DMPC- sHDL) exhibited a significantly ($p<0.05$) smaller hydrodynamic diameter than F1(DPPC-sHDL) or F2(SM-sHDL). The obtained results were in a good agreement with a study by Gong *et al*, where the average diameter of the blank DMPC-sHDL (12.58±0.34 nm) was smaller compared to sHDL prepared from other phospholipids. The difference in diameters was explained by the different phase transition temperatures of lipids which affects the fluidity of the lipid bilayer and its interaction with the peptide[17].

During the thermal cycling process, heating above the transition temperature of the lipids leads to fluidity of the lipid bilayer and facilitates the interaction with the peptide. Cooling, on the hand, renders the lipid membrane rigid and stable. Apparently, DMPC have a favorable transition temperature (T_m 23ºC) for the synthesis of sHDL since it occurs near the room temperature, and thus allows for association with the peptide, meanwhile preventing its dissociation from the membrane [17].

In formulas (F1-F9), the (lipids to peptide) ratio was varied from (2:1 to 1:1). Data depicted in table (3) and figure (2) revealed that altering the ratio from (2:1) to (1.5:1) caused a significant ($p<0.05$) decrease in the particles diameters. The obtained results imply the presence of more peptide to bind the lipid vesicles in (F4-F6) than in (F1-F3). However, further addition of peptide did not cause further size reduction; formulas (F7-F9) prepared with lipid to peptide ratio (1:1) exhibited significantly ($p<0.05$) increment in particle size compared to formulas prepared with (2:1) weight ratio, indicating the presence of large lipid vehicles and heterogeneity[34]. Previous studies have reported that the ability of a apolipoprotein or a peptide to bind lipids depends on its state of self-association. Efficient binding is achieved when the protein exists as monomers [32,35]. Therefore, at (1:1) ratio, the peptide molecules may exist as aggregates unable to adsorb and partition into lipid bilayers. The lipid-to-peptide weight ratio (1.5:1) was thus considered optimal for further investigation.

Among the nine formulas, F6 had the smallest particle size (159.8±8.6 nm); however, the desirable particle size of the ideal targeted nanocarrier (less than 100 nm) was not achieved.

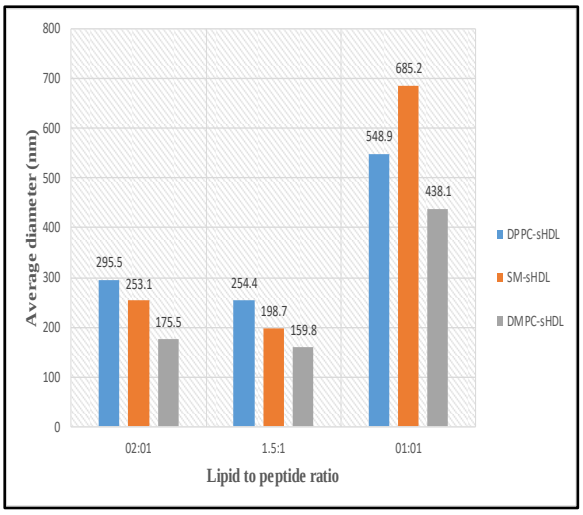

Figure 2. The effect of the lipid to peptide ratio on the average diameter of sHDL

Next, F10 and F11 were prepared by adding SM and DPPC, respectively into DMPC-based sHDL, accompanied by decreasing DMPC content so that the ratio of lipid to peptide was constant at (1.5:1). Adding SM significantly ($p<0.05$) decreased the particles diameter from 159.8±8.6 nm to 110.6±4.5 nm while DPPC exhibited opposite effect. SM which consists of a sphingosine backbone and phosphocholine head group was reported by Rye *et al* to increase packing order of the acyl chains and head groups in POPC-based discoidal HDL, therefore enabled the formation of smaller particles [36,37]. FESEM images of F10 showed the formation of nanodiscs as illustrated in figure (3).

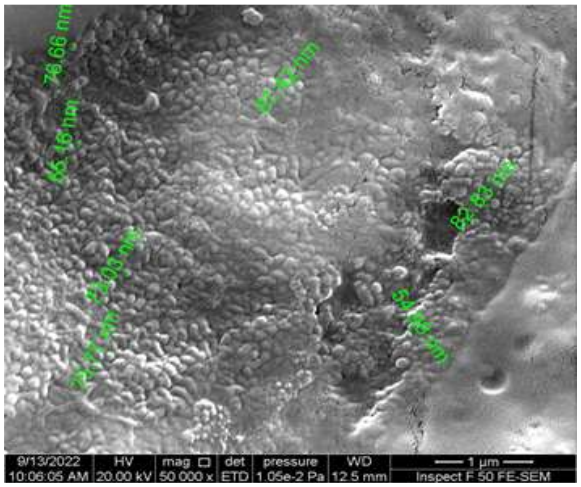

Figure 3. FESEM image of F10

It can be observed that the measured diameters of nanodiscs (figure 3) by FESEM were smaller than the average diameter obtained from DLS technique. The reason behind such difference lies in the method of sample preparation and the principles underlying each technique. The FESEM technique characterizes particles in dried state, while DLS measures the nanodiscs in solution, therefore measures the hydrodynamic diameter. DLS operate on the principle of light scattering, thus analysis is expected to bias towards larger particles because the intensity of scattered light is proportional to the sixth power of the diameter[38].

Zeta potential (ζ)

Zeta potential (ζ) represents the surface charge of nanoparticles. It is defined as the electrical potential at the boundary separating the tightly bound layer of solvent (shear plane) attached to the particles surface from the solution medium. The high absolute value of the ζ-potential will create repulsive electrostatic force between similarly charged particles in a dispersion and therefore will resist aggregation. Zeta potential analysis is important in predicting dispersions stability; a dispersion is considered stable when the absolute ζ-potential is 30mV or higher [39].

In addition to predicting stability, surface charge has a significant role in determining the biologic behavior and cellular uptake of nanoparticles. Cancer cells have a strong negative charge, therefore, they prefer to endocyte the positively charged nanoparticles. In receptor-ligand mediated targeting, the charge of the receptor's ligand binding site determines the affinity toward nanoparticles[40].With regard to SR-BI targeting, the active site of scavenger receptors encompasses a positively charged C-terminal of collagenous domain that enables a selective binding to negatively charged particles[41].The magnitude of ζ-potential of sHDL nanodiscs are presented in table (3). The values ranged from (-1.62±0.45 to -74.17±1.0) mV. The major components used in the preparation of sHDL nanodiscs are neutral molecules at pH 7.4; Phospholipids are zwitterions and neutral at the physiologic pH [42]. Likewise, the isoelectric point of 5A peptide is 6.75, thus it exhibits a net zero charge at physiological pH as shown in figure (4). Tamoxifen exists predominantly as positively charged form at the physiological pH, so the absence of positive surface charge can indicates the incorporation of tamoxifen molecules within the center of nanoparticles[43]. Consequently, the source of surface charge may result from adsorption of the salts used in the preparation.

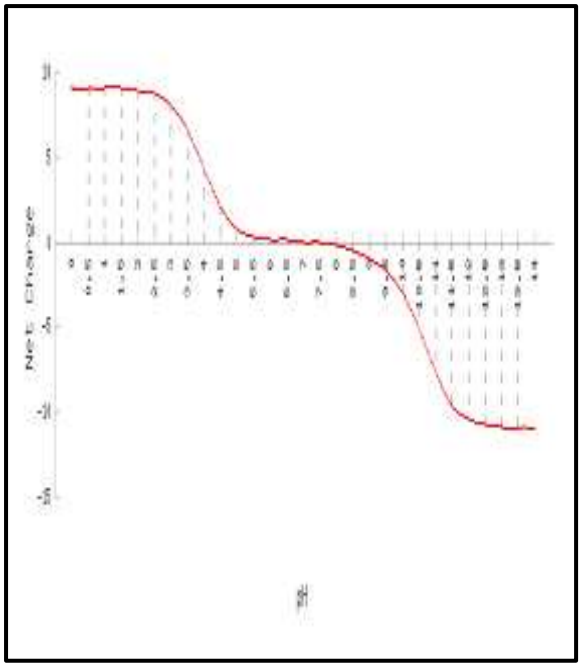

Figure 4. The net charge versus pH of 5 A peptide (provided by the manufacturing company, GenScript)

In vitro release of TC loaded sHDL nanodiscs

Tamoxifen citrate loaded sHDL nanoparticles are intended for intravenous administration; the optimized formulation should reveal minimum release of the encapsulated drug in blood circulation and maximum drug retention until they reaching cancer cells whereby the drug is transported into the cytoplasm of cancer cells through the non-aqueous "channel" of SR-B1 [12,15].

In order to study the influence of the phospholipid type on the release pattern of the drug from nanoparticles, *in vitro* release study was performed for formulas F4, F5, and F6 prepared using DPPC, SM and DMPC, respectively at fixed lipid to peptide ratio (1.5:1).

It was found that different lipids produced a significant effect ($P<0.05$) on the release pattern of TC from sHDL nanodiscs as shown in figure (5). Formula F6 containing DMPC with short acyl chain length (14 carbon atoms), and low T_m (23ºC) released the drug molecules faster than other formulas, mainly due to the fluidity of lipid bilayer at the physiological temperature (37ºC). On the other hand, F4 containing DPPC with 16 carbon atoms in acyl chain and transition temperature (41ºC) exhibited a slower release rate due to the rigidity against leakage of entraped molecules into release medium[44].

The release of TC from F5 was slower in comparison with other two formulas with 35.5 % of drug release by 24 hours. This can be attributed to the presence of hydrogen bond donors (N-H of the amide) and (O-H of shingosine);and hydrogen bond acceptors as C=O and phosphate group in sphingomyelin. As a result, sphingomyelin can form extensive intermolecular hydrogen bonding which increases the rigidity of the lipid bilayer [45]. Similar result was reported with docetaxel-sHDL nanodiscs, where SM-based sHDL retained more than 60 % of the drug followed by DPPC-based sHDL and DMPC-based sHDL[46].

Kuai R *et al* prepared sHDL from combined phospholipids of low T_m and the produced sHDL showed a relatively slow release of the drug from sHDL. sHDL nanodiscs loaded with withalongolide were prepared using DMPC and 1-palmitoyl-2-oleoyl-sn-glycero-3-phosphocholine (POPC) as the lipid composition[23]. Besides, one of the clinically tested HDL products in dyslipidemia, ETC-642, is composed of ApoA-I mimetic peptide /DPPC/SM at ratio (1:1:1)[47]. Therefore, F10 and F11 were prepared by adding SM or DPPC to DMPC-based sHDL.

It was observed that F10 and F11 exhibited a significant ($p<0.05$) slower release rate when compared to the release rate from F6. The incorporation of SM or DPPC with high T_m into DMPC-based sHDL may increase the order in the bilayer membrane than that of the pure DMPC-sHDL. As a result, sHDL prepared from combined phospholipids were less permeable to drug molecules. Villalaín *et al* studied the molecular interactions in phospholipids vesicles using differential scanning calorimetry (DSC) and FTIR. The mixture of SM and DPPC showed a transition temperature intermediate between those of individual lipids. In addition, the FTIR analysis showed that addition of SM decreased the motion and produced a more ordered acyl chains in the fluid state with respect to pure DPPC[48].

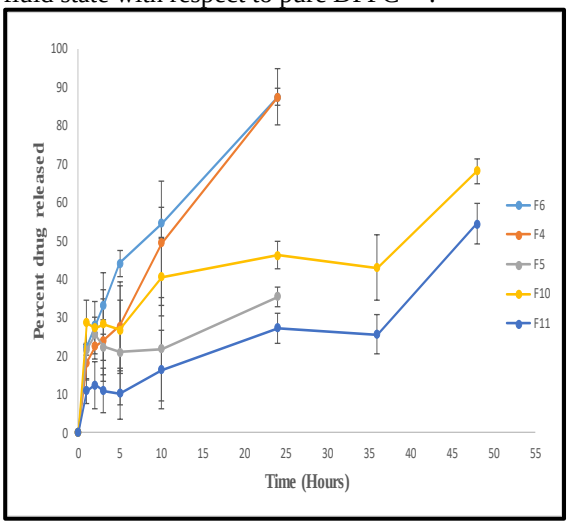

Figure 5. Effect of lipid type on the *in vitro* release profiles of TC from sHDL nanodiscs in PBS pH 7.4 at 37ºC. Each value represents the mean ± standard deviation (n=3)

Encapsulation efficiency (EE) and drug loading (DL)

Table 3 shows the values of EE and DL for sHDL nanodiscs (F1-F11). Sufficient encapsulation and drug loading are essential to obtain the desired therapeutic effect. The high EE and DL demonstrated by the sHDL nanodiscs could be attributed to the lipophilic nature of the drug (Log P 5.93) which enhances its encapsulation inside the lipid bilayer of sHDL[49].

Optimization and characterization of TC loaded-spherical sHDL

Formula F12 was prepared using egg yolk lecithin, FC, CO, and the mimetic peptide (5 A peptide) at lipid to peptide ratio of (2:1) and drug to carrier ratio of 0.2(w/w). The nanoparticles exhibited mean diameter of 77.7±5.7 nm and a narrow polydispersity index (0.005), which is favorable attributes for targeted nanocarrier. However, the drug release from nanoparticles shown in figure (6) exhibited an initial burst release, where 33.67% of TC released in the first hour followed by a slower release pattern. The burst release implies inefficient delivery of the therapeutic moiety to the target tissue and systemic toxicity, therefore it is undesirable in targeted delivery[50]. F13 was prepared by changing the lipid to peptide ratio to (1.5:1), resulting in a significant ($P<0.05$) increase in particle size, which may be due to the presence of peptide in aggregated state and the resulting in inefficient binding with phospholipids [34].

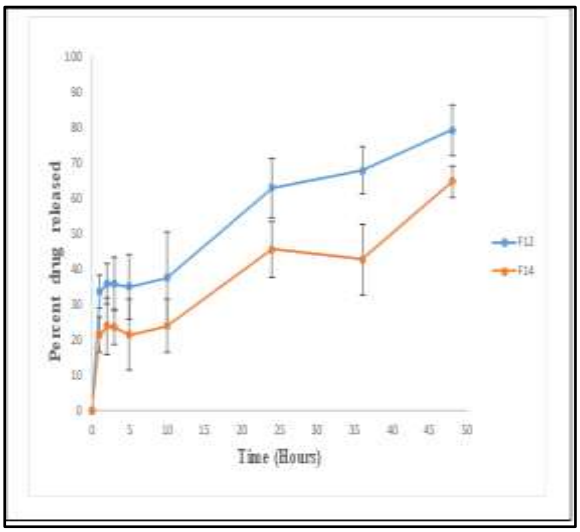

Figure 6. *In vitro* release profile of TC from F12 and F14 in PBS pH 7.4 at 37ºC. Each value represents the mean ± standard deviation (n = 3)
[4]

Next, Formula F14 was prepared to investigate the effect of other formulation parameters such as the drug to carrier ratio on the size and the drug release behavior from sHDL nanoparticles. With respect to the size of nanoparticles, a significant decrease ($p<0.05$) in the size of nanoparticles (from 77.7±5.7 to 35.7±12.4) nm was observed as the ratio decreased from 0.2 (w/w) to 0.1 (w/w). Because the drug molecules are encapsulated inside the hydrophobic core of nanoparticles, high drug to carrier ratio may cause the hydrocarbon chains of the phospholipid layer to become apart from each other [51]. FESEM images of F14 (figure 7) showed spherical shape nanoparticles in a nanosized range with a good correlation to the measurements obtained by DLS analysis.

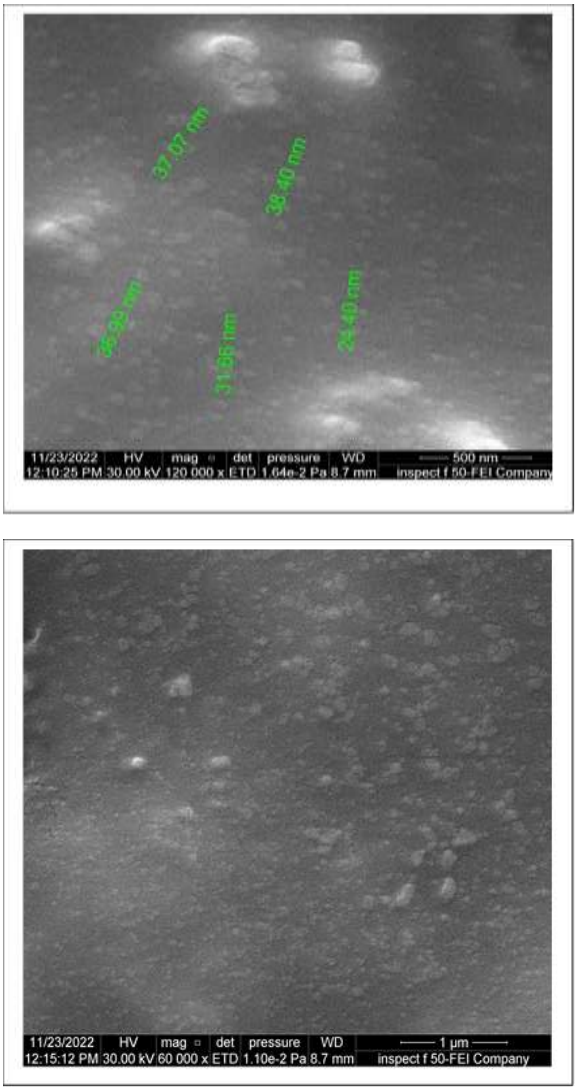

Figure 7. FESEM images of F14

In vitro release profiles of F12 and F14 displayed in figure (6) revealed that decreasing the drug to carrier ratio from 0.2 (w/w) to 0.1 (w/w) caused a significant ($p<0.05$) decrease in the release rate of TC from nanoparticles. The obtained observation was consistent with sHDL- mimicking nanodiscs loaded with docetaxel at 1.6% and 3.2% (46). Finding the optimal (drug to carrier ratio) is critical in determining the release behavior from sHDL. Lipophilic drugs like TC are encapsulated within the lipid membrane, and due to the relatively small

space to accommodate drug molecules, formulation of high drug to lipid ratio may disrupt the membrane integrity and eventually causes drug leakage. The total lipid concentration in F14 was increased and this lead to a considerable reduction in the burst release from sHDL nanoparticles[52].
Similarly, EE and DL were significantly increased by altering the drug to carrier ratio. Adding drug molecules in high concentration may exceed the capacity of the lipid membrane to house drug molecules; such overload can cause damage and leakage of drug molecules from the lipid membrane, and consequently low loading and encapsulation efficiency[52]).

Table 3 presents the values of ζ-potential of formulas (F12-F14). As discussed previously, the active drug, the phospholipid (egg yolk lecithin) and the peptide do not contribute to the surface charge whereas cholesterol and cholesteryl oleate do not carry ionizable functional groups. So, the surface charge was apparently acquired from adsorption of anions from the dispersion. F14 exhibited a value of (-48.4±0.5) mV, indicating a satisfactory stability attribute.

Analysis of the kinetics of drug release from sHDL nanoparticles

The release data of TC from F14 were fitted by different kinetic models including first order, zero order, Higuchi and Korsmeyer-Peppas models. The highest regression coefficient (R^2) was found for zero-order model (table 4), suggesting near zero order controlled mechanism. The hydrophobic core of sHDL nanoparticles restricted the drug molecules from the migration into the release medium. Furthermore, the peptide molecules at the surface of sHDL served as an effective barrier against drug diffusion. The obtained result was consistent with the result reported for lovastatin loaded hyaluronic acid - decorated reconstituted high density lipoprotein [53].

Table 4. *In Vitro* Release Kinetic Data of TC from F14

Model	R^2
Zero-order model	0.9217
First-order model	0.8924
Higuchi model	0.8633
Korsmeyer–Peppas	0.5796

Colloidal stability in human plasma

The optimized formula F14 was incubated in human plasma to simulate the physiologic conditions that sHDL may encounter in blood stream. The adsorption of plasma proteins on the surface of sHDL may cause aggregation of the nanoparticles, increase in particle size, changes in surface charge and enhances their clearance. Furthermore, the adsorbed proteins and enzymes especially lecithin cholesterol acyltransferase (LCAT) enzyme can disrupt the lipid membrane of sHDL nanoparticles, and eventually resulting in drug leakage. Therefore, monitoring the changes in mean particles size and zeta potential is important to evaluate the stability in the presence of plasma [54].

In this study, no sign of aggregation or sedimentation was observed after incubation for 24 hours with plasma. The mean particle size showed a significant ($p<0.05$) increase from 35.7±8.8 nm to 90.4±10 nm. In addition, the value of zeta potential has altered from -48.4±0.5 to -73.9±1.3 mV as a result of adsorption of plasma proteins. However, the particle size did not exceed 100 nm, indicating good stability under physiologic conditions [15].

Powder x-ray diffraction (PXRD)

The PXRD patterns of the raw materials TC, 5A, lecithin and the optimized formula F14 are shown in figure (8). TC exhibited sharp peaks indicated the crystalline nature of the drug. The main diffraction peaks of TC appeared at a diffraction angle of 2θ at 5.77º, 12.92º, 13.98º, 15.14º, 17.3º, 19.81º, 21.01º, 24.18º and 28.28º. Lecithin also showed sharp peaks indicating crystallinity while the halo in the spectrum of 5A reflects its amorphous nature. The absence of characteristic peaks of TC from the diffractograms of the optimized formula, F14, suggests a molecular distribution of drug molecule within the lipid membrane of sHDL nanoparticles. Similar finding was reported for tamoxifen and resveratrol layer-by-layer nanoparticles [55]. In addition, the diffraction peaks of the lecithin were weakened and shifted in F14 mainly due to formation of a less ordered crystals than in bulk lipids [56].

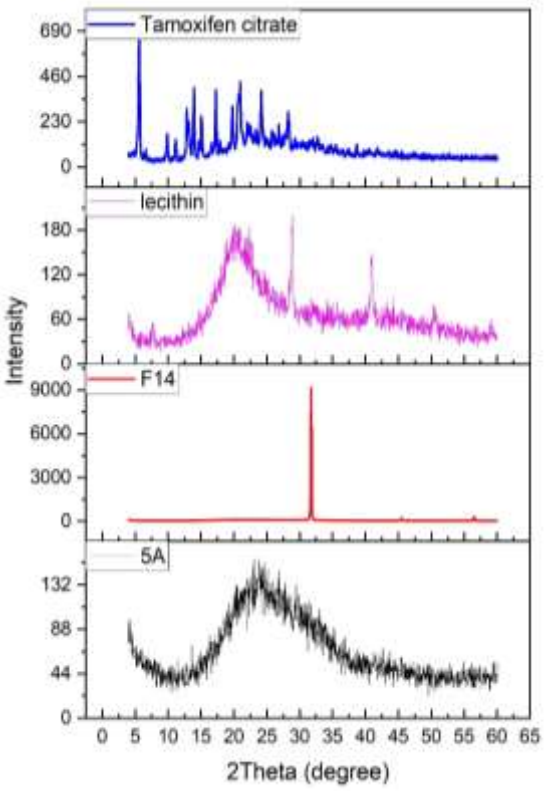

Figure 8. The PXRD patterns of TC, lecithin, F14 and 5A

Fourier transform infrared (FTIR) spectroscopy

Figure (9) demonstrates the characteristic bands of the TC, namely 3402.43 cm^{-1} due to N-H stretching vibrations, 1589.34 cm^{-1} assigned to N-H bending, 1238.3 cm^{-1} due to asymmetric C-O-C stretch, 1172.72 cm^{-1} due to C-N stretch and 1739.79 cm^{-1} assigned to carbonyl group of the citrate salt. It shows the aromatic C-H stretching band at 3020.53 cm^{-1}, and the ring C-C stretching bands at 1504.48 cm^{-1} and 1438.9 cm^{-1}. In addition, the spectrum shows the aliphatic asymmetric C-H stretching at 2974.23 cm^{-1} and symmetric C-H stretching at 2870.08 cm^{-1}. The spectrum of the prepared formula, F14, recorded a shift in N-H stretching band of TC to a lower frequency, suggesting the formation of hydrogen bonds with the carrier components. The absence of shift in peak positions for other principal peaks of the drug implies the absence of chemical interaction between the drug and excipients. FTIR spectra include bands, amide I (around 1655 cm^{-1}) due to carbonyl group of the peptide backbone, and amide II (around 1546 cm^{-1}) due to N-H bending. The aforementioned bands provide information on the helical conformation which promotes the lipid binding. Therefore, the appearance of these bands in the spectrum of the F14 indicates that the peptide association with the lipid membrane did not cause structural change to the peptide molecule [57].

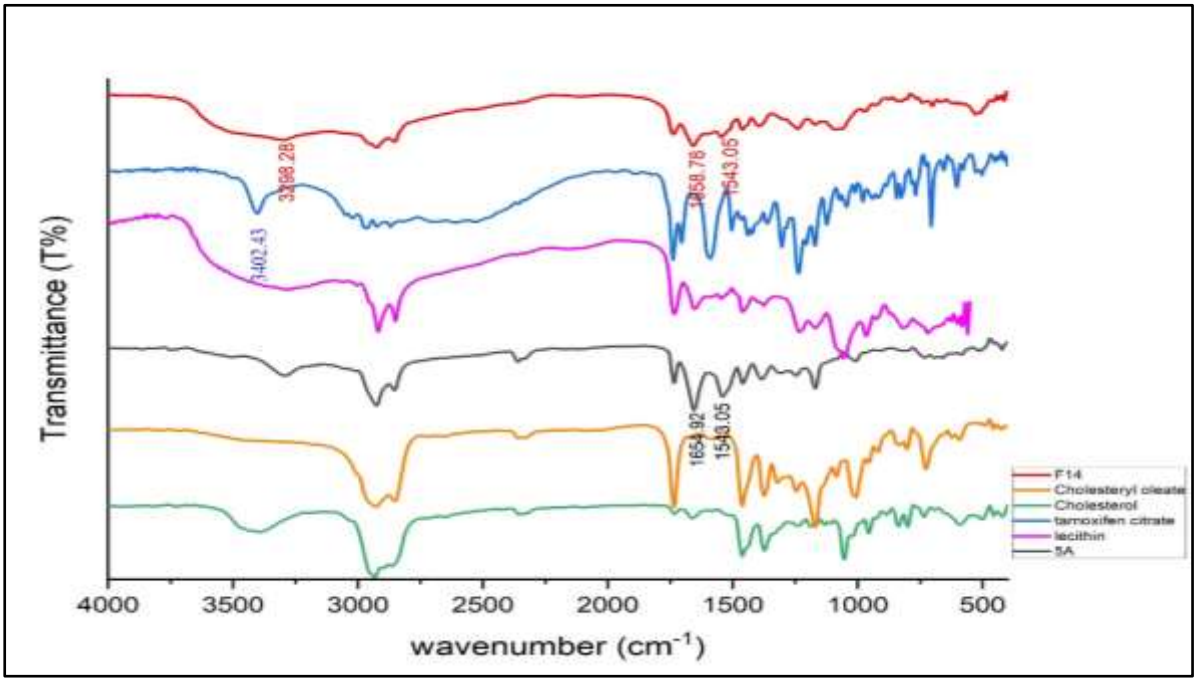

Figure 9. FTIR spectra for 5A, lecithin, TC, cholesterol, cholesteryl oleate, F14

Conclusion

From the results of this study, it was found that it is possible to develop and optimize synthetic high density lipoproteins (sHDL) loaded with TC. The optimized formula (F14) was prepared using (egg yolk

lecithin:FC:CO:5A) at 2:1 lipid to peptide ratio and 0.1 (w/w) drug to carrier ratio. The average diameter, PDI, release pattern and colloidal stability studies indicate the feasibility of the prepared sHDL nanoparticles as a targeted drug delivery system for intravenous administration.

Acknowledgments

The authors are thankful to department of Pharmaceutics/ Collage of Pharmacy-University of Mustansiriyah (www.uomustansiriyah.edu.iq), Baghdad–Iraq. Authors are also grateful to the staff of Center of Nanotechnology and Advanced Research-University of Technology for their assistance to accomplish this study.

Conflicts of Interest

Authors declare no conflict of interests.

References

1. Jahan S, Karim ME, Chowdhury EH. Nanoparticles targeting receptors on breast cancer for efficient delivery of chemotherapeutics. Biomedicines. 2021;9(2):1–30.

2. Higa G. Breast Cancer. In: Chisholm-Burns MA, Schwinghammer TL, Wells BG, Malone PM, Kolesar JM, DiPiro JT, editors. Pharmacotherapy Principles & Practice. Fourth edi. New York: MC Graw Hill Education; 2016. p. 1321–2.

3. British Pharmacopoeia Commission. British Pharmacopoeia. London: The Stationery Office; 2009.

4. Mircioiu I, Anuta V, Ibrahim N, Mircioiu C. Dissolution of tamoxifen in biorelevant media. A two phase release model. Farmacia. 2012;60(3):315–24.

5. O'Neil M, editor. The Merck Index: An Encyclopedia of Chemicals,Drugs,and Biologicals. 14 th edit. New Jersey: merck; 2006.

6. Day CM, Hickey SM, Song Y, Plush SE, Garg S. Novel tamoxifen nanoformulations for improving breast cancer treatment: Old wine in new bottles. Molecules. 2020;25(5).

7. Schiff R, Chamness GC, Brown PH. Advances in breast cancer treatment and prevention: Preclinical studies on aromatase inhibitors and new selective estrogen receptor modulators (SERMs). Breast Cancer Res. 2003;5(5):228–31.

8. British National Formulary (BNF). BMJ Group and the Royal Pharmaceutical Society of Great Britain; 2021. 997 p.

9. Ghaidaa S. Hameed, Methaq Hamad Sabar. Nano-carriers as a Selective Treatment for Cancer. Al Mustansiriyah J Pharm Sci. 2021;21(1):55–66.

10. Kuai R, Li D, Chen YE, Moon JJ, Schwendeman A. High-Density Lipoproteins: Nature's Multifunctional Nanoparticles. ACS Nano. 2016;10(3):3015–41.

11. Zhang X, Huang G. Synthetic lipoprotein as nano-material vehicle in the targeted drug delivery. Drug Deliv. 2017;24(0):16–21.

12. Ma X, Song Q, Gao X. Reconstituted high-density lipoproteins: novel biomimetic nanocarriers for drug delivery. Acta Pharm Sin B. 2018;8(1):51–63.

13. Gupta A, Sharma R, Kuche K, Jain S. Exploring the therapeutic potential of the bioinspired reconstituted high density lipoprotein nanostructures. Int J Pharm. 2021;596:120272.

14. Mei Y, Tang L, Xiao Q, Zhang Z, Zhang Z, Zang J, et al. Reconstituted high density lipoprotein (rHDL), a versatile drug delivery nanoplatform for tumor targeted therapy. J Mater Chem B. 2021;9(3):612–33.

15. Fazel M, Daeihamed M, Osouli M, Almasi A, Haeri A, Dadashzadeh S. Preparation, in-vitro characterization and pharmacokinetic evaluation of brij decorated doxorubicin liposomes as a potential nanocarrier for cancer therapy. Iran J Pharm Res. 2018;17(Special Issue 2):33–43.

16. Rocha M, Chaves N, Báo S. Nanobiotechnology for Breast Cancer Treatment. In: Pham P Van, editor. Breast cancer – From Biology to Medicine. London, UK: IntechOpen; 2017. p. 13.

17. Gong M, Zhang Q, Zhao Q, Zheng J, Li Y, Wang S, et al. Development of synthetic high-density lipoprotein-based ApoA-I mimetic peptide-loaded docetaxel as a drug delivery nanocarrier for breast cancer chemotherapy. Drug Deliv. 2019;26(1):708–16.

18. Abed HN, Hussein AA. Ex-vivo absorption study of a novel dabigatran etexilate loaded nanostructured lipid carrier using non-everted intestinal sac model. Iraqi J Pharm Sci. 2019;28(2):37–45.

19. Bondarenko L, Terekhova V, Kahru A, Dzhardimalieva G, Kelbysheva E, Tropskaya N, et al. Sample preparation considerations for surface and crystalline properties and ecotoxicity of bare and silica-coated magnetite nanoparticles. RSC Adv. 2021;11:32227–35.

20. Raval N, Maheshwari R, Kalyane D, Youngren-Ortiz SR, Chougule MB, Tekade RK. Importance of physicochemical characterization of nanoparticles in pharmaceutical product development. Basic Fundamentals of Drug Delivery. Elsevier Inc.; 2018. 369–400 p.

21. Danışman-Kalındemirtaş F, Kariper İA, Erdemir G, Sert E, Erdem-Kuruca S. Evaluation of anticancer effects of carboplatin–gelatin nanoparticles in different sizes synthesized with newly self-assembly method by exposure to IR light. Sci Rep. 2022;12(1):10686.

22. Sahib AS, Alhammid SNA, Akrami M, Muhammed HA. Preparation and in-vitro hematological evaluation of chlorambucil loaded lipid nanoparticles. Int J Drug Deliv Technol. 2021;11(3):850–7.

23. Kuai R, Subramanian C, White PT, Timmermann BN, Moon JJ, Cohen MS, et al. Synthetic high-density lipoprotein nanodisks for targeted withalongolide delivery to adrenocortical carcinoma. Int J Nanomedicine. 2017;12:6581–94.

24. Safavi MS, Shojaosadati SA, Dorkoosh FA, Jo HJ, Kwon Y, Lee KC, et al. The synthesis of tamoxifen-loaded albumin nanoparticles by homogenizers: Optimization and in vitro characterization [Internet]. Vol. 41, Journal of Drug Delivery Science and Technology. Elsevier Ltd; 2017. 20–30 p. Available from: http://dx.doi.org/10.1016/j.jddst.2017.06.007

25. Yu X, Sun L, Tan L, Wang M, Ren X, Pi J, et al. Preparation and Characterization of PLGA–PEG–PLGA Nanoparticles Containing Salidroside and Tamoxifen for Breast Cancer Therapy. AAPS PharmSciTech. 2020;21(3):85.

26. Heidari Majd M, Akbarzadeh A, Sargazi A. Evaluation of host–guest system to enhance the tamoxifen efficiency. Artif Cells, Nanomedicine Biotechnol. 2017;45(3):441–7.

27. Allah AKA, Hussein AA. Preparation and evaluation of darifenacin hydrobromide loaded nanostructured lipid carriers for oral administration. Iraqi J Pharm Sci. 2018;27(1):53–68.

28. Salman ZD, Alhamdany AT, Yousif NZ. An innovative mucoadhesive thermosensitive in situ gelling liquid suppository of metoclopramide hydrocloride for treatment of nausea and vomiting associated with diseases. Indian J Pharm Sci. 2020;82(4):650–64.

29. Katas H, Hussain Z, Awang SA. Bovine serum albumin-loaded chitosan/dextran nanoparticles: Preparation and evaluation of ex vivo colloidal stability in serum. J Nanomater. 2013;2013:1–9.

30. Jaafar IS, Radhi AA. preparation-and-physicochemical-characterization-of-cocrystals-for-enhancing-the-dissolution-rate-.pdf. J Adv Pharm Edu Res. 2020;10(3):68–76.

31. Mohammad HA, Ghareeb MM, Akrami M, Sahib AS. Design and characterization of Tacrolimus monohydrate loaded core shell lipid polymer hybrid nanoparticle. J Complement Med Res. 2020;11(5):204–14.

32. Patel H, Ding B, Ernst K, Shen L, Yuan W, Tang J, et al. Characterization of apolipoprotein A-I peptide phospholipid interaction and its effect on HDL nanodisc assembly. Int J Nanomedicine. 2019;14:3069–86.

33. Yuan Y, Wen J, Tang J, Kan Q, Ackermann R, Olsen K, et al. Synthetic high-density lipoproteins for delivery of 10-hydroxycamptothecin. Int J Nanomedicine. 2016;11:6229–38.

34. Tang J, Li D, Drake L, Yuan W, Deschaine S, Morin EE, et al. Influence of route of administration and lipidation of apolipoprotein A-I peptide on pharmacokinetics and cholesterol mobilization. J Lipid Res. 2017;58(1):124–36.

35. Pittman RC, Glass CK, Atkinson D, Small DM. Synthetic high density lipoprotein particles. Application to studies of the apoprotein specificity for selective uptake of cholesterol esters. J Biol Chem. 1987;262(6):2435–42.

36. Martínez-Beamonte R, Lou-Bonafonte JM, Martínez-Gracia M V., Osada J. Sphingomyelin in High-Density Lipoproteins: Structural Role and Biological Function. Int J Mol Sci. 2013;14(4):7716–41.

37. Rye KA, Hime NJ, Barter PJ. The influence of sphingomyelin on the structure and function of reconstituted high density lipoproteines. J Biol Chem. 1996;271(8):4243–50.

38. Maguire CM, Rösslein M, Wick P, Prina-Mello A. Characterisation of particles in solution–a perspective on light scattering and comparative technologies. Sci Technol Adv Mater. 2018;19(1):732–45.

39. Ramírez-García G, Trapiella-Alfonso L, D'Orlyé F, D'Orlyé A. Electrophoretic methods for characterizing nanoparticles and evaluating their bio-interactions for their further use as diagnostic, imaging, or therapeutic tools. In: Colin F. Poole, editor. Handbooks in Separation Science, Capillary Electromigration Separation Methods. Elsevier; 2018. p. 397–421.

40. Saadat M, Zahednezhad F, Zakeri-Milani P, Heidari HR, Shahbazi-Mojarrad J, Valizadeh H. Drug targeting strategies based on charge dependent uptake of nanoparticles into cancer cells. J Pharm Pharm Sci. 2019;22(1):191–220.

41. Lokhande AS, Jahagirdar P, Dandekar P, Devarajan PV. Scavenger Receptor and Targeting Strategies. In: Devarajan P, Dandekar P, D'Souza A, editors. Targeted Intracellular Drug Delivery by Receptor Mediated Endocytosis. AAPS Advances in the

Pharmaceutical Sciences Series, vol 39. Springer, Cham.; 2019.
42. Blanco A, Blanco G. 05 - Lipids. In: Blanco A, Blanco G, editors. Medical Biochemistry. Academic Press; 2017. p. 99–119.
43. Vakili-ghartavol R, Rezayat SM, Faridi-majidi R, Sadri K. Optimization of Docetaxel Loading Conditions in Liposomes : proposing potential products for metastatic breast carcinoma chemotherapy. Sci Rep. 2020;10:5569.
44. Anderson M, Omri A. The Effect of Different Lipid Components on the In Vitro Stability and Release Kinetics of Liposome Formulations The Effect of Different Lipid Components on the In Vitro Stability and Release Kinetics of Liposome Formulations. Drug Deliv. 2004;11(1):33–9.
45. Mady MM. Serum stability of non-cationic liposomes used for DNA delivery. Rom J Biophys. 2004;14(June 2005):89–97.
46. Kadiyala P, Li D, Nunez FM, Altshuler D, Doherty R, Kuai R, et al. High-Density Lipoprotein-Mimicking Nanodiscs for Chemo-immunotherapy against Glioblastoma Multiforme. ACS Nano. 2019;13(2):1365–84.
47. Di Bartolo BA, Vanags LZ, Tan JT, Bao S, Rye KA, Barter PJ, et al. The apolipoprotein A-I mimetic peptide, ETC-642, reduces chronic vascular inflammation in the rabbit. Lipids Health Dis. 2011;10(1):224.
48. Villalaín J, Ortiz A, Gómez-Fernández JC. Molecular interactions between sphingomyelin and phosphatidylcholine in phospholipid vesicles. BBA - Biomembr. 1988;941(1):55–62.
49. Gu X, Zhang W, Liu J, Shaw JP, Shen Y, Xu Y, et al. Preparation and characterization of a lovastatin-loaded protein-free nanostructured lipid carrier resembling high-density lipoprotein and evaluation of its targeting to foam cells. AAPS PharmSciTech. 2011;12(4):1200–8.
50. Kafshgari MH, Khorram M, Khodadoost M, Khavari S. Reinforcement of Chitosan Nanoparticles Obtained by an Ionic Cross-linking Process. Syria Stud. 2011;20(5):445–56.
51. Nasrollahi Z, Khani S, Amani A. Ratio of Drug/carrier as dominant factor in determining size of doxorubicin-loaded Beta-1,3- Glucan Nanoparticles: A study using artificial neural networks. Nanomedicine Res J. 2020;5(2):114–9.
52. Chountoulesi M, Naziris N, Pippa N, Demetzos C. The significance of drug-to-lipid ratio to the development of optimized liposomal formulation. J Liposome Res. 2018;28(3):249–58.
53. Liu L, He H, Zhang M, Zhang S, Zhang W, Liu J. Hyaluronic acid-decorated reconstituted high density lipoprotein targeting atherosclerotic lesions. Biomaterials. 2014;35(27):8002–14.
54. Zhang F, Wang X, Xu X, Li M, Zhou J, Wang W. Reconstituted high density lipoprotein mediated targeted co-delivery of HZ08 and paclitaxel enhances the efficacy of paclitaxel in multidrug-resistant MCF-7 breast cancer cells. Eur J Pharm Sci. 2016;92:11–21.
55. Al-Jubori AA, Sulaiman GM, Tawfeeq AT, Mohammed HA, Khan RA, Mohammed SAA. Layer-by-layer nanoparticles of tamoxifen and resveratrol for dual drug delivery system and potential triple-negative breast cancer treatment. Pharmaceutics. 2021;13(7).
56. Babaei S, Ghanbarzadeh S, Adib ZM, Kouhsoltani M, Davaran S, Hamishehkar H. Enhanced skin penetration of lidocaine through encapsulation into nanoethosomes and nanostructured lipid carriers: A comparative study. Pharmazie. 2016;71(5):247–51.
57. Mady MM, Elshemey WM. Interaction of dipalmitoyl phosphatidylcholine (DPPC) liposomes and insulin. Mol Phys An Int J Interface Between Chem Phys. 2011;109(12):1593–8.